

The effect of hydrodynamics on the mass transfer of dissolved inorganic carbon to the freshwater macrophyte *Vallisneria americana*

Gregory N. Nishihara

Department of Integrative Biology, University of Guelph, Guelph, Ontario N1G 2W1, Canada

Josef D. Ackerman¹

Department of Integrative Biology and Faculty of Environmental Sciences, University of Guelph, Guelph, Ontario N1G 2W1, Canada

Abstract

The combined effects of water velocity (U) and dissolved inorganic carbon (DIC) concentration on photosynthesis rates of *Vallisneria americana* were investigated. The net photosynthesis rate or O_2 flux (J_{obs}) from leaves increased with U from 0.20 ± 0.01 (mean \pm standard error) $\mu\text{mol m}^{-2} \text{s}^{-1}$ at $U = 0 \text{ m s}^{-1}$ (i.e., in stagnant water) to $2.1 \pm 0.07 \mu\text{mol m}^{-2} \text{s}^{-1}$ at $U = 0.066 \text{ m s}^{-1}$. The velocity where J_{obs} was saturated (U_{sat}) was inversely proportional to the DIC concentration ([DIC]) and decreased monotonically from $0.04 \pm 0.01 \text{ m s}^{-1}$ at 0.46 mol m^{-3} to $0.006 \pm 0.004 \text{ m s}^{-1}$ at 4.8 mol m^{-3} . If the net photosynthesis rate and DIC uptake are equal, HCO_3^- uptake rates contributed $>90\%$ of DIC uptake at all [DIC] at $U = 0.005 \text{ m s}^{-1}$ and contributed less at higher velocities. The proportion of HCO_3^- uptake to DIC uptake decreased linearly with increasing [DIC]. The measured local Sherwood numbers (Sh_x) and the parameter a (2.24 ± 1.32) for O_2 of the equation, $Sh_x = a Re_x^b Sc^{0.33}$ were higher than predicted for a laminar flat plate boundary layer, indicating that physicochemical activity, such as photosynthesis, influenced Sh_x . The thickness of the measured concentration boundary layer (δ_{CBL}) and the diffusive sublayer (δ_{DSL}) were 63% and 70% smaller, respectively, than theoretical values based on hydrodynamic theory. Theoretical hydrodynamic predictions of mass transfer need to account for biological reactions.

The water column serves as the primary source and sink for dissolved nutrients, gases, and by-products produced and consumed by aquatic organisms (Okubo et al. 2002; Lorke et al. 2003; Larned et al. 2004). The mass transfer of these solutes is a complex process, and aside from diffusion, the transport of solutes to and from the water column and organisms is affected by water velocity, solute concentration, chemical reactions, and the geometry of the organism (Riebesell et al. 1993; Larned et al. 2004; Falter et al. 2005). Hence, the ecophysiology of aquatic organisms is directly influenced by the surrounding environment and the rates of mass transfer have a profound influence on processes such as photosynthesis, respiration, and nutrient uptake (Ploug et al. 1999, 1999, 2002). In the case of photosynthetic organisms, Sanford and Crawford (2000) have proposed that the control of nutrient uptake can be categorized into three regimes: (1) mass transfer limited, where the nutrient uptake rate increases proportionally to increases in the rates of mass transfer; (2) kinetically limited, where little or no change in the uptake rate occurs with increases in the rates of mass transfer; or (3) both, i.e., an intermediate regime, where both the rates of mass transfer and kinetics

are important. Indeed, increasing mass transfer rates has been shown to enhance nutrient uptake in periphyton (Larned et al. 2004), corals (Thomas and Atkinson 1997), macroalgae (Hurd et al. 1996), and seagrasses (Thomas et al. 2000). However, the degree of enhancement may vary with the nutrient and uptake mechanism, as for example, in the seagrass *Thalassia testudinum*, where under the same hydrodynamic regime, ammonium uptake was mass transfer limited, whereas nitrate uptake was kinetically limited (Cornelisen and Thomas 2004).

Mass transfer rates depend on water velocity (U) and nutrient concentration (C), and, in general, an increase in water velocity or nutrient concentration will increase the rates of mass transfer. However, such increases do not necessarily enhance; they can also inhibit physiological processes. For example, this occurs through the reconfiguration of the shape of the organism, which minimizes drag but also decreases the surface area available for nutrient uptake, light capture, and photosynthesis (Stewart and Carpenter 2003); through mechanical stress that can impair and reduce photosynthesis rates (Madsen and Søndergaard 1983; Koch 1993); or by removing cations, protons, or extracellular carbonic anhydrase that facilitate nutrient uptake or photosynthesis (Borchardt et al. 1994; Flores-Moya and Fernández 1998).

Dissolved inorganic carbon (DIC) is considered to be in limiting concentrations in the aquatic environment (Madsen and Sand-Jensen 1991; Madsen et al. 1996). Indeed, for obligate CO_2 users, DIC is limiting (Madsen and Sand-Jensen 1991; Riebesell et al. 1993); however, for species able to use HCO_3^- , DIC may exist in saturating concentrations

¹ Corresponding author (ackerman@uoguelph.ca).

Acknowledgments

The authors would like to thank Patrick Ragaz and Mark Loewen for assistance with the PIV and two anonymous reviewers for their comments on the manuscript.

This research was supported in part by funding from the University of Guelph and the Natural Sciences and Engineering Research Council of Canada to J.D.A.

(Tortell et al. 1997; Tortell and Morel 2002). Moreover, DIC limitation is also dependent on temperature, nutrients, and light (Madsen et al. 1996), and where these variables are not limiting, physical variables such as morphology, pH, water velocity, and DIC concentration ([DIC]) (Hurd 2000) as well as biological features such as carbon concentrating mechanisms (Madsen and Maberly 2002; Raven 2003), may further enhance carbon supply for photosynthesis. As mentioned previously, water velocity will enhance the nutrient delivery to an organism and enhance nutrient uptake rates. Whereas there are examples of U or [DIC] enhanced DIC uptake by macrophytes (Wheeler 1980; Invers et al. 2001), little is known on the combined effects of water velocity and DIC concentrations on photosynthesis.

The freshwater angiosperm, *Vallisneria americana*, is a convenient model species in which to investigate how U and DIC affect photosynthesis. *V. americana* has long flat ribbon-like leaves that grow submerged or lie along the water surface and is found in stagnant and fast flowing freshwater environments in eastern North America, where it can grow to >2 m in length (Catling et al. 1994). The flat ribbon-like shape of the leaves provides a good model to compare to mass transfer theory developed for flat plates. In addition, *V. americana* is known to use HCO_3^- as a DIC source for photosynthesis (Titus and Stone 1982), providing an opportunity to examine the interaction of U and [DIC] on mass transfer.

Mass transfer theory—The observed O_2 flux (J_{obs}), or the net photosynthesis rate, can be modeled as the sum of O_2 flux under diffusive (J_{diff}) and advective (J_{adv}) conditions.

$$J_{obs} = J_{diff} + J_{adv} \quad (1)$$

Photosynthesis can occur through J_{diff} alone (i.e., at $U = 0 \text{ m s}^{-1}$) (Wheeler 1980; Koch 1993), however, under advection, J_{obs} exhibits a positive slope and attains a maximum O_2 flux (J_{max}) at large U (a relationship that can be described by a rectangular hyperbola) beyond which at some critical velocity (U_{crit}), photosynthesis rates may decline (Madsen and Søndergaard 1983; Koch 1993; Stewart and Carpenter 2003). Therefore, J_{adv} can be separated into a component that describes the enhancing effects of increasing U up to some saturating velocity (U_{sat}), where U_{sat} is the velocity at which J_{obs} is 90% J_{max} ; a component where J_{obs} remains constant; and a third component that describes the inhibitory effect of $U > U_{crit}$ where photosynthesis declines

$$J_{adv} = \frac{J_{max}U}{V+U} - f(M,P,U,U_{crit}) \quad (2)$$

where V is the velocity at $0.5 J_{max}$ (note that $U_{sat} = 9V$), and M and P are characteristics of plant morphology and physiology, respectively (Fig. 1).

In the analogy for flow over a flat plate, mass transfer occurs through a momentum boundary layer (BL) of thickness (δ) at some distance (x) downstream of a leading edge. The BL is initially laminar, in which viscous forces predominate, and becomes turbulent at a critical local

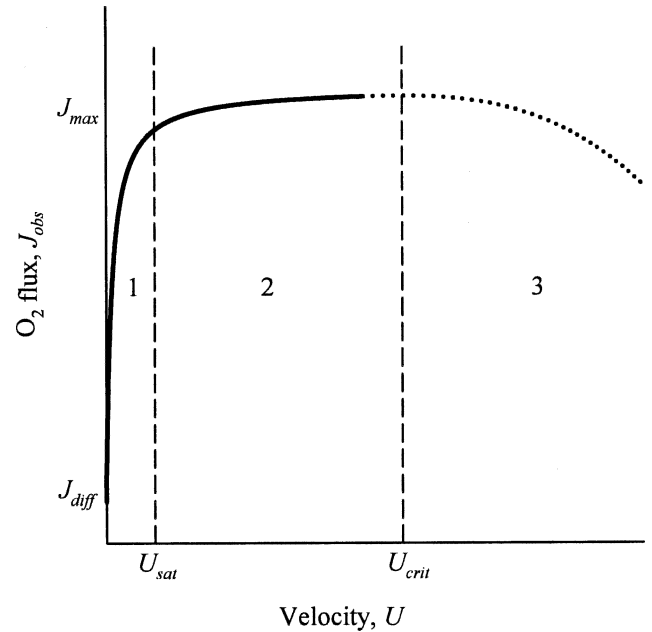


Fig. 1. Model of the influence of velocity on photosynthetic rates of aquatic plants given by $J_{obs} = J_{diff} + \frac{J_{max}U}{V+U} - f(M,P,U,U_{crit})$, where J_{obs} is the observed O_2 flux, J_{diff} is the O_2 flux at a velocity (U) of 0 m s^{-1} , J_{max} is the maximum O_2 flux, V is the velocity at $0.5 J_{max}$, U_{crit} is the velocity where the inhibitory effects of increasing U decreases O_2 flux, and M and P are the characteristics of the plant morphology and physiology, respectively. O_2 flux increases when U is less than U_{sat} in region 1, O_2 flux is insensitive to further increases of U in region 2 (where $U_{sat} < U < U_{crit}$), and O_2 flux decreases when $U > U_{crit}$ in region 3 as indicated by the dotted line.

Reynolds number, Re_x (where $Re_x = xU/\nu$ and ν is the kinematic viscosity). The turbulent BL can be separated into three regions: the outer region, the logarithmic sublayer, and the viscous sublayer (VSL). The effects of viscosity are greatest adjacent to the leaf surface in the relatively thin VSL (e.g., Okubo et al. 2002). If a concentration gradient exists between the surface and the water column, a concentration boundary layer (CBL) forms with a smaller diffusive sublayer (DSL) adjacent to the leaf surface (e.g., Okubo et al. 2002; Nishihara and Ackerman 2006). The CBL, in two-dimensions at steady-state, is directly influenced by the momentum BL, since the velocity terms (u , w) in the downstream (x) and vertical (z) directions are components of the advection–diffusion–reaction equation for mass transfer (Bird et al. 2002)

$$u \frac{\partial C}{\partial x} + w \frac{\partial C}{\partial z} = \frac{\partial}{\partial z} \left((D + K_D) \frac{\partial C}{\partial z} \right) + R \quad (3)$$

where D and K_D are the molecular and turbulent diffusivity of the solute, and R describes any reaction occurring in the CBL. The mass transfer from a surface can then be characterized by the local Sherwood number (Sh_x), which is the ratio of advective to diffusive mass flux, given by

$$Sh_x = aRe_x^b Sc^{0.33} \quad (4)$$

where a is an empirical coefficient that is influenced by the orientation and geometry of the leaf surface (Schuepp 1993) and reactions occurring within or as a boundary condition of the CBL (Bird et al. 2002). It is important to note that Schuepp (1993) indicated that the mass flux was constant over a thin leaf from a terrestrial plant and that the local Sherwood number varied with the local boundary layer thickness (c.f., Schlichting and Gersten 2000). In cases for a laminar boundary layer of a flat plate where $R = 0$, a has a value of 0.464 at constant mass flux from the local surface and 0.339 at constant surface concentration (Schlichting and Gersten 2000). The parameter b approaches 0.5 for laminar boundary layers or 0.8 if the boundary layer is turbulent (Schuepp 1993). Sc is the Schmidt number, which is the ratio of the molecular diffusivity of momentum (ν) to the molecular diffusivity of the solute (D). Sh_x can also be interpreted as a dimensionless local mass transfer coefficient

$$Sh_x = \frac{K_c x}{D} \quad (5)$$

where K_c is the local mass transfer coefficient (dimensions of $L T^{-1}$) and is a function of the water, the surface geometry of the leaf, and the conditions of flow. K_c for O_2 can be determined from the shape of the O_2 profile in the CBL at steady-state by evaluating Fick's first law of diffusion at the leaf surface

$$K_c(C_s - C_b) = -D \left. \frac{dC}{dz} \right|_{z=0} \quad (6)$$

where C_s and C_b are the concentrations at the leaf surface and in the bulk water, respectively, and flux is positive away from the leaf surface. It should also be possible to determine Sh_x and K_c for DIC (CO_2 and HCO_3^-) after measuring K_c and a and b in Eq. 4 for O_2 by using the appropriate value of Sc in Eq. 4 (Bird et al. 2002).

In cases where there is no water flow, O_2 concentrations accumulate at the leaf surface, and the system is no longer at steady-state. In this situation, J_{obs} can be estimated by using Fick's second law of diffusion, with respect to time (t), for an infinite plane source evaluated at the surface ($z = 0$) (Basmadjian 2003) given by

$$C = J_{diff} \left(\frac{t}{\pi D} \right)^{1/2} \Big|_{z=0} \quad (7)$$

The objective of this study is to determine how physical forcing and the interaction between U and [DIC] affect J_{obs} and how well mass transfer theory applies to J_{obs} .

Materials and methods

V. americana, obtained from Boreal Laboratories, were grown on a soil substrate in 20-liter aquaria at 25°C. The diel cycle was set to 16 : 8 light : dark (LD) and a 4π sensor (QSL2101, Biospherical Instruments) determined that

the photosynthetically active radiation (PAR), 0.10 m below the water surface, was 7.3 μmol photon m⁻² s⁻¹. Local well water was used for cultivation and was enriched with 30 mol m⁻³ NO₃⁻, 40 mol m⁻³ SO₄⁻, and 1,100 mol m⁻³ K⁺. To discourage algae growth, no PO₄⁻ was added.

Experimental setup—A 10 × 10 × 100-cm-long flow chamber with flow straighteners in the upper 12 cm was used to conduct experiments (Fig. 2A). The flow chamber was operated at average velocities (U) of 0.005, 0.008, 0.011, 0.018, 0.021, 0.033, 0.041, and 0.066 m s⁻¹ as determined by volumetric measurements corresponding to Re_{dh} ranging from 667 to 7,158 (based on the hydraulic diameter of the chamber; water depth ~5.5 cm). Velocity profiles observed in the empty flume 0.56 m downstream of the flow straighteners (location of the leading edge of a leaf) were determined with a digital particle image velocimetry (PIV) system. The profiles were logarithmic and uniform in shape above a height of 0.03 m, where the leaves were located, indicating well behaved flow conditions (see *Particle image velocimetry*) (Fig. 2B). Bulk water was aerated to maintain O_2 (263 mmol m⁻³) and recirculated by a submersible pump. The water temperature was kept at 24°C, and the initial pH was adjusted with sodium hydroxide pellets. The pH remained stable during the experiments (9.2 ± 0.2 (mean ± standard error); note that the high pH observed during this study is characteristic of the local groundwater source. Additional experiments indicated that there was no effect of aeration on pH (i.e., stable [CO₂] and [HCO₃⁻] during a typical time frame of an experiment (4–6 h), even at the lowest [DIC]. Bulk O_2 was measured with an OXN oxygen microsensor (Unisense).

An OX25 oxygen microsensor (Unisense; tip diameter = 25 μm) was used to measure the O_2 profile in the CBL by attaching it to a motorized micromanipulator with a vertical resolution of 0.010 mm that was positioned $x = 0.025$ m from the leading edge of the leaf (0.56 m downstream of the flow straighteners). The microsensors were connected to a picoammeter (PA2000, Unisense), and the O_2 , bulk pH, and water temperature were logged continuously to a computer with a data acquisition device (PMD-1208LS, Measurement Computing). A slide projector equipped with a quartz lamp (82V; 300W; General Electric) was used as a light source and PAR was measured 3 cm above the flow chamber bottom with a 4π sensor (QSL2101, Biospherical Instruments). Preliminary experiments indicated that high PAR levels inhibited photosynthesis, therefore neutral density filters were used to attenuate PAR. However, since subsaturating PAR may dampen the effects of U on photosynthesis (Wheeler 1980; Koch 1993), attenuation was controlled to ensure that 153 μmol photon m⁻² s⁻¹ was used during all experiments.

Leaves were carefully selected from the culture that satisfied the following criteria: (1) they were relatively flat without undulations along the length or width; (2) they were not covered with visible epiphytes; and (3) they could provide a 7-cm-long section for the experiment. After selection, leaves were cut to size and placed in the reservoir

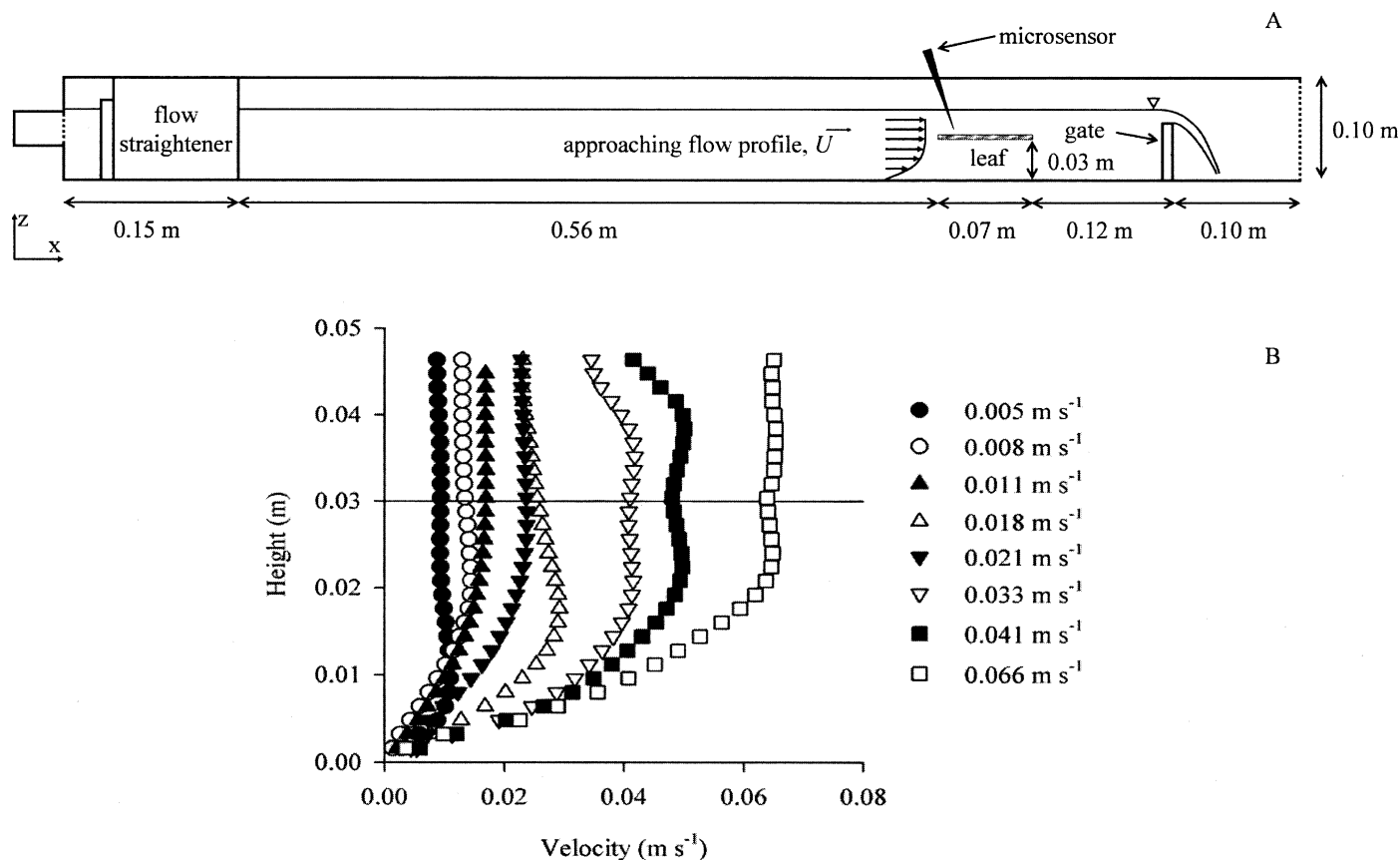


Fig. 2. (A) Diagram of the recirculating flow chamber used to determine the influence of mass flux on the photosynthesis of *V. americana* leaves as measured by profiling of the O_2 concentration boundary layer. (B) Velocity profiles of the approaching flow measured in an empty flow chamber, where the solid horizontal line indicates the position of the leaf at $z = 0.03$ m.

to acclimate overnight. Leaf sections averaged 0.7 ± 0.03 cm wide and were attached to a wire stand with cyanoacrylate-based glue. The leaf and stand were placed in the working section of the flow chamber, 0.56 m downstream from the flow straighteners, perpendicular to the light source, and parallel to the flow.

As there were no changes in bulk water O_2 during an experiment, the O_2 measured during profiling was converted to % O_2 saturation by dividing the measured voltage by the voltage obtained when the microsensor was furthest from the leaf surface in the bulk water, where O_2 concentration was at saturation (note that the microsensor response is linear in this range; Glud et al. 1994; Lorenzen et al. 1995). The % O_2 saturation was converted to molar concentration by multiplying by the solubility of oxygen in freshwater at 24°C (i.e., 263 mmol m^{-3}).

Calculating O_2 flux— J_{obs} at the leaf surface can be calculated using Fick's first law,

$$J_{obs} = -D \left. \frac{dC}{dz} \right|_{z=0} \quad (8)$$

where J_{obs} is evaluated at the leaf surface ($z = 0$). A recent treatment indicates that advective flux also occurred in the CBL, and because the concentration gradient is nonlinear,

J_{obs} is best determined by fitting a hyperbolic tangent to a dimensionless concentration gradient (θ) (Nishihara and Ackerman 2006). This concentration gradient (θ) is determined from

$$\theta = \frac{C_s - C}{C_s - C_b} \quad (9)$$

Where the local values of $\theta(z)$ can be modeled as

$$\theta(z) = B \tanh\left(\frac{A}{B} z\right) \quad (10)$$

The derivative of Eq. 10 is evaluated at $z = 0$

$$\left. \frac{d\theta}{dz} \right|_{z=0} = A \quad (11)$$

since

$$\left. \frac{dC}{dz} \right|_{z=0} = A(C_s - C_b) \quad (12)$$

and J_{obs} can be calculated as

$$J_{obs} = DA(C_s - C_b) \quad (13)$$

where A is a parameter of $\theta(z)$.

Velocity and DIC concentration effects—The effect of U and [DIC] on J_{obs} were investigated by profiling the concentration of O_2 above *V. americana* leaves. The OX25 was carefully positioned over the leaf surface, and measurements were made after adjusting the position of the OX25 tip from $z = 0.000$ to 0.200 mm (in 0.020 -mm steps), 0.200 to 1.000 mm (in 0.100 -mm steps), 2.000 mm, and 3.000 mm. J_{obs} was calculated with the hyperbolic tangent model (Eqs. 9 to 13) with the initial position, $z = 0$, offset after adjustments. Profiling was undertaken twice for each of six leaves at eight U (0.005 to 0.066 m s⁻¹) and a given [DIC] (0.46 , 1.0 , 1.8 , 2.5 , 3.7 , and 4.8 mol m⁻³); i.e., a total of 36 leaves were used. [DIC] was adjusted by mixing appropriate volumes of deionized water and tap water, which was obtained from local groundwater and has a pH of 9.2 ± 0.2 and a $[HCO_3^-]$ of 4.8 ± 0.1 mol m⁻³ (i.e., before addition of nutrients and NaOH during the experiments). At the six combinations of [DIC], pH remained stable during the experiments, and the HCO_3^- to CO_2 ratios were > 600 to 1 . The CO_2 concentrations estimated from the Henderson–Hasselbalch equation for open systems ranged from 0.34 mmol m⁻³ at the lowest [DIC] to 5.8 mmol m⁻³ at the highest [DIC] (Stumm and Morgan 1996).

Mass transfer analyses—Local mass transfer coefficients for O_2 were calculated by solving for K_c in Eq. 6, where D for O_2 is 2.4×10^{-9} m² s⁻¹ at $24^\circ C$. Sh_x was calculated for O_2 using Eq. 5, where x was 0.025 m downstream of the leading edge of the leaf. The parameters a and b in Eq. 4 were determined by plotting a semi-log plot of Eq. 4 as a linear regression (i.e., $Sh_x/Sc^{0.33}$ vs. $\log Re_x$, where $a =$ intercept and $b =$ slope). The CBL thickness (δ_{CBL}) is the distance from the leaf surface to where the O_2 concentration is 99% of the bulk concentration as determined from Eq. 10. The DSL thickness (δ_{DSL}) is found by taking the first derivative of Eq. 10 and extrapolating the slope at $z = 0$ to the distance where the slope intercepts the value of the bulk O_2 concentration (Hondzo et al. 2005).

Particle image velocimetry—Vertical profiles of the velocity field in an empty flume and above the leaves were obtained through the use of a PIV system (Nishizaki and Ackerman 2005). In the latter case, the laser light sheet was directed from above to intersect the leaf in the mid-longitudinal plane. Silver-coated hollow glass beads ($13\text{-}\mu\text{m}$ diameter) were suspended in the flow, and a digital video camera captured their images at a frequency of 30 Hz through the side wall of the flow chamber. A total of 150 frames were obtained and processed in a 768×481 pixel grid with an 80×80 pixel interrogation window. The velocity records 0.006 m upstream and downstream of $x = 0.025$ m (or 0.56 m downstream of the flow straighteners in the case of the flow chamber profiles) were averaged for each height above the leaf surface to provide a velocity profile. The shear velocities (u_*) were obtained by multiplying the von Karman constant ($\kappa = 0.41$) by the slope of the velocity versus $\ln(z)$ in the logarithmic portion of the boundary layer (Ackerman and Hoover 2001).

O_2 flux in stagnant water—A $95 \times 75 \times 60$ mm glass chamber was placed in the flume to ensure the physical conditions were similar to those with water movement. Care was taken to prevent flume water from entering the glass chamber and causing water motion. The OX25 was carefully positioned over the leaf surface ($z = 0$) while viewing through a dissecting microscope. The light source was turned off, and the O_2 concentration was allowed to decrease. After several minutes, the light source was turned on (153 $\mu\text{mol photon m}^{-2} \text{s}^{-1}$), and the data was immediately recorded to a computer at 5 Hz for 12 minutes. Six leaves were evaluated at each of two concentrations of HCO_3^- (1.2 and 4.8 mol m⁻³). J_{diff} was estimated from Eq. 7 by nonlinear regression.

Water quality—The pH and alkalinity of the bulk water used for the experiments in the glass chamber and the flow chamber were analyzed to estimate HCO_3^- concentrations. The aerated bulk water was titrated with 0.02 mol m⁻³ hydrochloric acid (HCl) to determine the alkalinity (American Water Works Association 1998).

Statistical analyses—Statistica 6.1 (Statsoft, Inc.) was used for all analyses. Linear and nonlinear regressions were used to analyze the appropriate data. The 95% confidence region of the parameters determined for the nonlinear regression of J_{obs} with respect to U and the F statistic with a Bonferroni's correction ($\alpha = 0.003$, 15 comparisons) was used to compare among the six HCO_3^- concentrations (Mead et al. 2003). All t -tests were evaluated at $\alpha = 0.05$, and values in the text are reported as the mean \pm standard error. The standard errors from the nonlinear regressions are asymptotic unless stated otherwise.

Results

In stagnant water, J_{obs} at 1.2 and 4.8 mol m⁻³ DIC were similar (0.20 ± 0.03 and 0.021 ± 0.03 $\mu\text{mol m}^{-2} \text{s}^{-1}$, respectively; $t_{10} = 2.22$, $p = 0.88$) and the average of the two is used as an estimate of J_{diff} throughout the report. The response of J_{obs} to U followed a saturation-like pattern whereby small increases in U at the lowest velocities led to large increases in J_{obs} up to a maximum (J_{max}) after which point (U_{sat}) increases in U had little effect on J_{obs} (Fig. 3). The pattern was evident for all [DIC], and the rectangular hyperbolic function described by the first term in Eq. 2 yielded significant fits ($p < 0.001$) to the data, which were significantly different among [DIC] (Bonferroni corrected F -test, $p < 0.001$). Two additional patterns were evident. First, J_{max} ranged from 1.1 $\mu\text{mol m}^{-2} \text{s}^{-1}$ to 2.1 $\mu\text{mol m}^{-2} \text{s}^{-1}$ with no apparent trend with respect to [DIC] and averaged 1.50 ± 0.14 $\mu\text{mol m}^{-2} \text{s}^{-1}$ (Figs. 3, 4). Second, U_{sat} decreased significantly with [DIC] (Figs. 3, 4), from 0.04 ± 0.01 m s⁻¹ at 0.46 mol m⁻³ to 0.006 ± 0.004 m s⁻¹ at 4.8 mol m⁻³ (regression: $U_{sat} = 0.046 \pm 0.003 - (0.008 \pm 0.001)$ [DIC]; $r^2 = 0.91$; $p < 0.001$). J_{obs} were similar to those observed in an earlier study on *V. americana* (Nishihara and Ackerman 2006) and in studies of other aquatic macrophytes (e.g., Madsen and

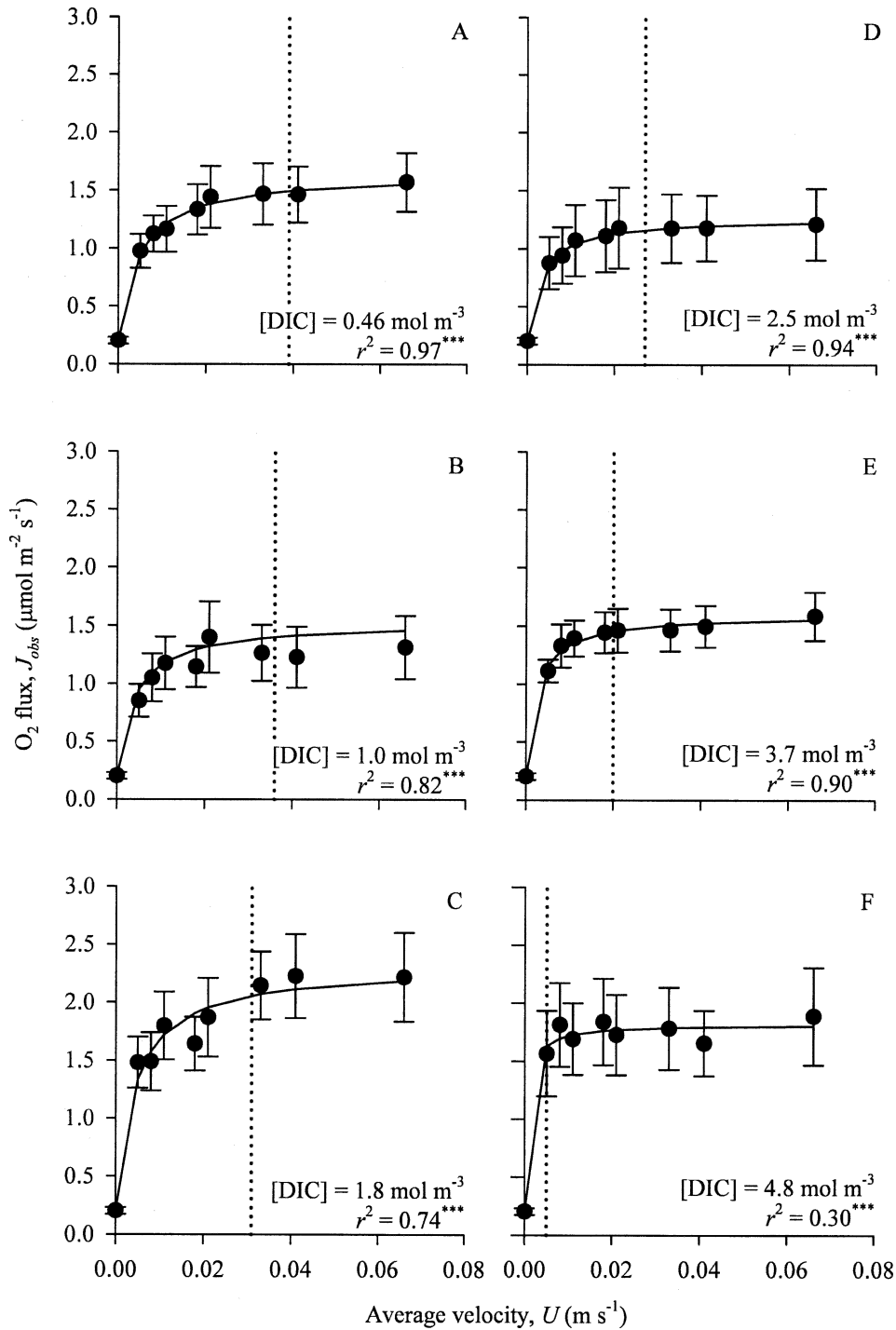


Fig. 3. The effects of the water velocity (U) on O₂ flux (J_{obs}) in *V. americana* at six [DIC]. Solid lines indicate the fitted model, the dotted vertical line indicates the location of the saturation velocity (U_{sat}), and the bars indicate standard error. $n =$ six leaves for each DIC concentration where the flux is the average from two profiles each. *** indicates $p < 0.001$.

Sand-Jensen 1991) when normalized to chlorophyll *a+b* content.

The mass transfer (Sh_x) of O₂ increased monotonically with Re_x (in this case U was varied and x was constant), and the range of Sh_x values increased with Re_x (Fig. 5). As above, it was not possible to segregate the Sh_x according to

[DIC]. In all cases, the experimentally determined Sh_x were considerably larger than the prediction from flat plate theory. In this case, the empirically fit data averaged 470% \pm 18% larger than the theoretical prediction of Sh_x (solid line in Fig. 5). The estimate of the parameter a in Eq. 4 was also much larger than flat plate theory (2.24 ± 1.32 (mean

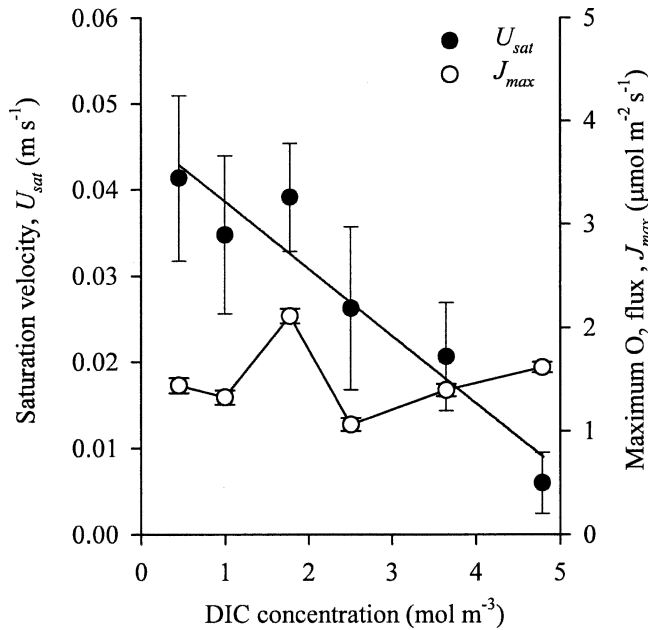


Fig. 4. The effect of [DIC] on the saturation velocity (U_{sat}) and maximum O_2 flux (J_{max}) in *V. americana*. Error bars indicate asymptotic standard errors from a nonlinear regression. $n =$ six leaves with two profiles each. Regression line: $U_{sat} = 0.0464 \pm 0.0033 - (0.0078 \pm 0.0012)$ [DIC]; $r^2 = 0.91$; $p < 0.001$.

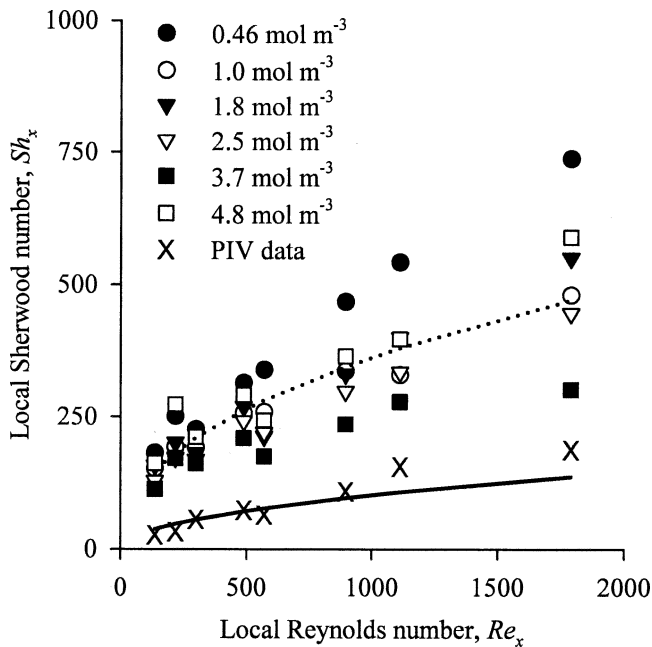


Fig. 5. The local Sherwood number (Sh_x) for O_2 mass transfer with respect to the local Reynolds number (Re_x) of a *V. americana* leaf. The dotted line indicates the empirical equation fitted to the measured data, $Sh_x = 2.24 Re_x^{0.45} Sc^{0.33}$, and the solid line is the theoretical Sh_x for a flat plate with constant surface flux ($Sh_x = 0.464 Re_x^{0.5} Sc^{0.33}$). Sh_x calculated from local mass transfer coefficients estimated using the velocity profile data and $K_c = 0.1u_*Sc^{-0.67}$ (Dade 1993).

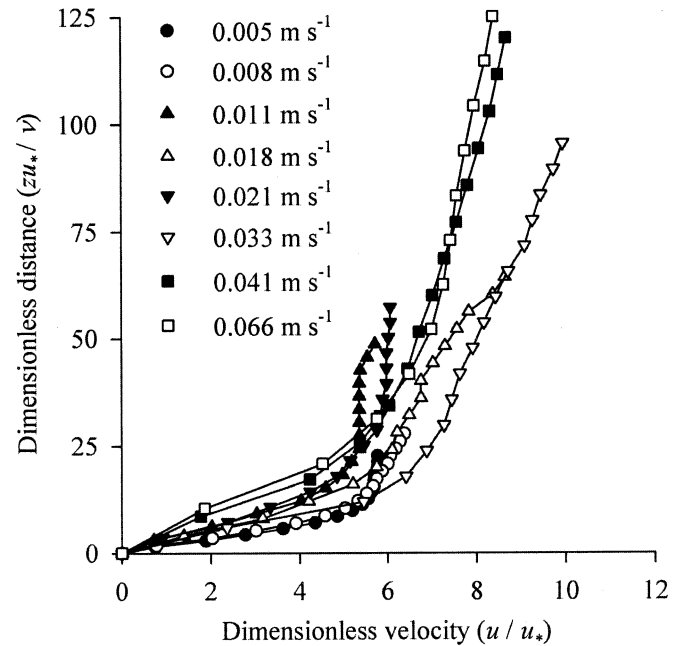


Fig. 6. The dimensionless velocity profiles within the momentum BL across the surface of a *V. americana* leaf at a distance $x = 0.025$ m downstream from the leading edge. Symbols as in Fig. 2B.

$\pm 95\%$ CI) vs. 0.464 for constant surface flux), but the exponent b was similar for laminar flow over a flat plate (0.45 ± 0.04 vs. 0.5; Schuepp 1993).

The velocity profiles measured above the *V. americana* leaf positioned in mid-channel and mid-depth (Fig. 6) had a logarithmic profile and were similar to the profiles observed in the empty flume (Fig. 2B), which indicated the presence of a momentum boundary layer at all U (Fig. 6). The profiles at the lowest U tended to be steeper at $U/u_* \approx 5$, relative to the profiles of the higher velocities. It was possible to determine u_* values for each profile ($r^2 > 0.93$; $p < 0.001$ in all cases). The u_* values were 1.3 ± 0.1 mm s^{-1} at 0.005 m s^{-1} , 1.6 ± 0.1 mm s^{-1} at 0.008 m s^{-1} , 2.8 ± 0.1 mm s^{-1} at 0.011 m s^{-1} , 3.9 ± 0.1 mm s^{-1} at 0.018 m s^{-1} , 3.3 ± 0.1 mm s^{-1} at 0.021 m s^{-1} , 5.9 ± 0.7 mm s^{-1} at 0.033 m s^{-1} , 8.6 ± 0.6 mm s^{-1} at 0.041 m s^{-1} , and 11.3 ± 0.8 mm s^{-1} at 0.066 m s^{-1} . The shear velocity determined from the momentum BL (Fig. 6), can be used to provide an independent estimate of Sh_x provided in Eq. 5

$$K_c = 0.1u_*Sc^{-0.67} \quad (14)$$

(Dade 1993). The Sh_x determined from the PIV data were similar in magnitude to the predictions of flat plate theory, especially at lower Re_x . Moreover, their distribution was strongly correlated with the flat plate theory ($r^2 = 0.95$; $p < 0.001$, Fig. 5). As evident in the large value of a , the ratio of J_{adv} to J_{diff} appears to be much greater for *V. americana* than what is predicted for constant surface flux to a flat plate.

Given that the CO_2 concentration at the surface is zero (Prins et al. 1980), the CO_2 uptake rate can be estimated

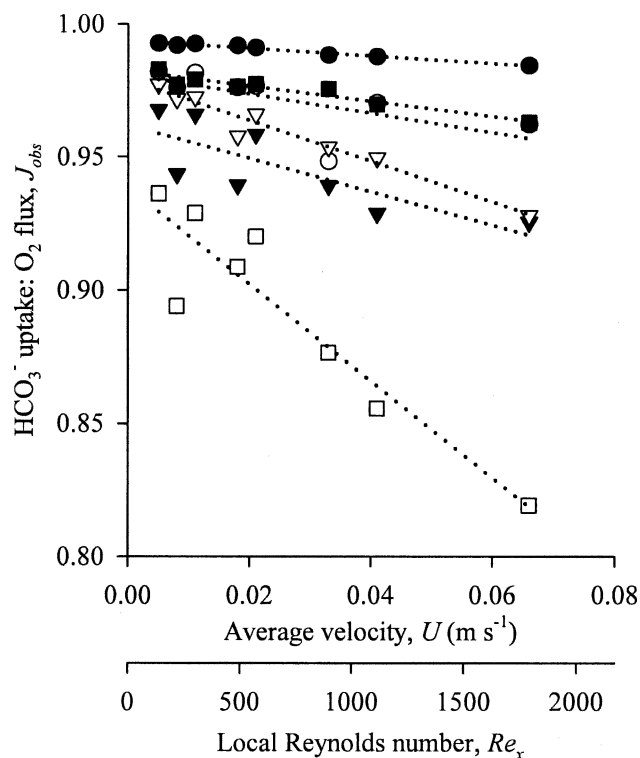


Fig. 7. The proportion of O_2 flux (J_{obs}) attributed to HCO_3^- uptake rates of *V. americana* with increases in water velocity (U). The dotted lines are linear regressions to the data, where r^2 were all significant ($p < 0.05$) and >0.70 . Symbols and conventions as in Fig. 5.

from the Sh_x of CO_2 , and the HCO_3^- uptake rate is the difference between the total DIC uptake and CO_2 uptake rates. As can be seen in Fig. 7, at low U (0.005 m s^{-1}), HCO_3^- uptake rates represented $>90\%$ of all DIC uptake at all [DIC] (recall that the pH during the experiments was 9.2 ± 0.2). The relative contribution of HCO_3^- uptake to J_{obs} decreased monotonically with U , but the rates varied among [DIC]. There was some evidence that CO_2 uptake was related to high [DIC], but this relationship was not strong (Fig. 7).

The HCO_3^- concentration at the leaf surface was estimated from the HCO_3^- uptake rates and mass transfer coefficient. In this case, the ratio of the leaf surface to the bulk water HCO_3^- concentration ($C_s : C_b$) with respect to U is given in Fig. 8. The $C_s : C_b$ ratio increased nonlinearly with increasing U , and the increase was greatest at the lowest [DIC] (0.46 mol m^{-3}). Where [DIC] were relatively large (i.e., $>2.5 \text{ mol m}^{-3}$), the change in $C_s : C_b$ with respect to U was small.

The thickness of the CBL (δ_{CBL}) and the DSL (δ_{DSL}) can be compared and contrasted between empirical measurement of O_2 and the hydrodynamic models using the parameters estimated from the PIV (Fig. 9). The empirical and theoretical δ_{CBL} and δ_{DSL} decreased with increases in U . The measured δ_{CBL} was about 63% thinner than the hydrodynamic δ_{CBL} determined from flat plate theory given by $\delta_{CBL} = 5 \times Re_x^{-0.5} Sc^{-0.33}$. Similarly, the empirical δ_{DSL} was about 70% thinner than the theoretical values

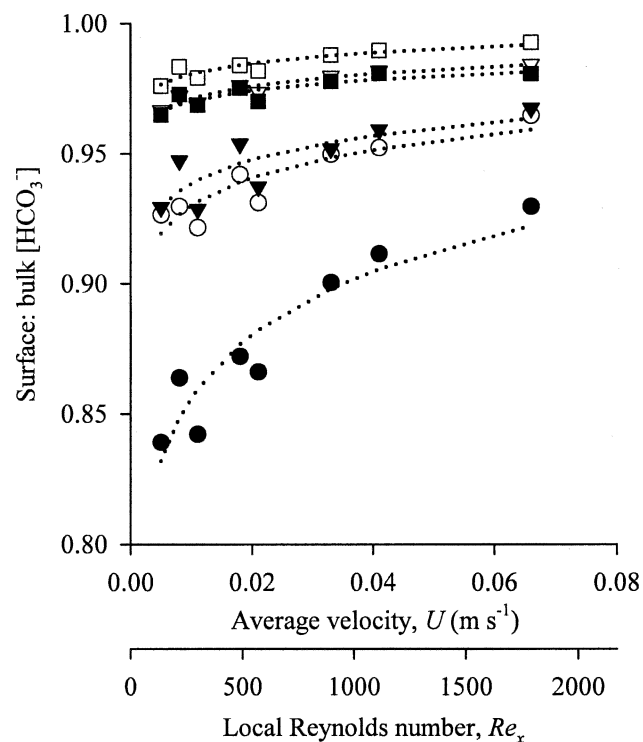


Fig. 8. The change in HCO_3^- surface concentration (C_s) to bulk concentration (C_b) ratio with increasing water velocity (U) for *V. americana*. Dotted lines indicate fitted logarithmic regressions. Symbols and conventions as in Fig. 5.

given by $\delta_{DSL} = 10 (v/u_*) (v/D)^{-0.33}$ (Dade 1993; Lorke et al. 2003). It is evident that estimates of δ_{CBL} and δ_{DSL} from flat plate boundary layer theory overestimates the thicknesses observed around *V. americana* leaves.

Discussion

Water velocity and DIC—Both U and [DIC] are important factors that affect the mass transfer of solutes for *V. americana*. In this study, increasing U from 0 to 0.066 m s^{-1} enhanced J_{obs} regardless of the [DIC] (Fig. 3). The enhancement of J_{obs} by U was also observed for the freshwater angiosperm *Callitriche stagnalis* (Madsen and Søndergaard 1983) and the marine macroalgae *Ulva lactuca* (Koch 1993) and *Macrocystis pyrifera* (Wheeler 1980). Similarly, the uptake rates of ammonium, nitrate, and phosphorus were also enhanced by increasing U for corals (Thomas and Atkinson 1997), seagrasses (Thomas et al. 2000), macroalgae (Hurd et al. 1997), and periphyton (Larned et al. 2004). However, no relationship was apparent for J_{max} when [DIC] were increased from 0.46 mol m^{-3} to 4.8 mol m^{-3} , which indicates that [DIC] used in this study were not limiting for the *V. americana* leaves when $U > U_{sat}$.

At a given nutrient concentration, the increases in uptake rates and photosynthesis are directly related to the increase in U through the changes in the momentum and concentration boundary layers and the associated changes in mass transfer rates (Bird et al. 2002). By increasing U , the velocity gradient increases, and this increases the

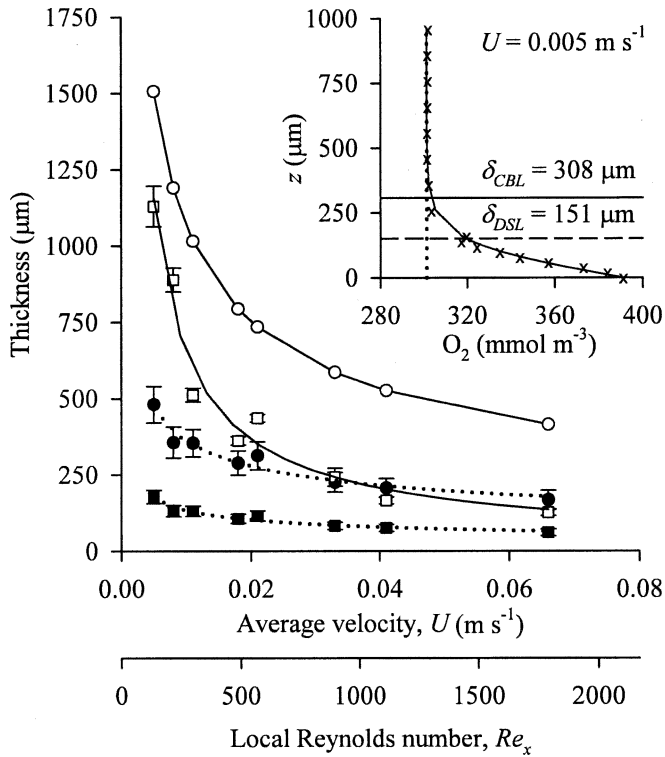


Fig. 9. The thickness (δ) of the CBL and the DSL of O_2 above a *V. americana* leaf. The theoretical δ_{CBL} (open circle) is based on the hydrodynamics of a flat plate and is given by $\delta_{CBL} = 5 \times Re_x^{-0.5} Sc^{-0.33}$ (Bird et al. 2002), and the measured δ_{CBL} is based on the hyperbolic tangent model (closed circle) applied to the O_2 measurements, where δ_{CBL} is the distance from the surface where the O_2 concentration is 99% of the bulk value. The theoretical δ_{DSL} (open square) estimated from hydrodynamic measurements is given by $\delta_{DSL} = 10 \nu/u^* (v/D)^{-0.33}$ (Dade 1993; Lorke et al. 2003), and the measured δ_{DSL} thickness (closed square) is from the first derivative of the hyperbolic tangent model. The inset shows an example of the hyperbolic tangent model fit to an O_2 profile at 0.005 m s^{-1} and indicates the measured δ_{CBL} and δ_{DSL} . Error bars indicate standard error.

concentration gradient, which enhances mass transfer to the surface of an organism. However, the effect of U becomes less important at high nutrient concentrations, where a large potential is created by the difference in concentrations, which also increases the concentration gradient (Sanford and Crawford 2000). By increasing the mass transfer of nutrients through increases in nutrient concentration, the effect of U on mass transfer is less important, as is evident in this study where increasing [DIC] lowered the U_{sat} (Figs. 3, 4). The enhancing effects of U on mass transfer were more evident at lower [DIC] as has also been observed in coral reefs for ammonium uptake, when nutrient concentrations were low but U were high (Thomas and Atkinson 1997).

To better understand how U and [DIC] influence J_{obs} consider a simple example. In this case, the same bulk mass flux of $0.024 \text{ mol m}^{-2} \text{ s}^{-1}$ is provided by $U = 0.050 \text{ m s}^{-1}$ and [DIC] = 0.048 mol m^{-3} and by $U = 0.005 \text{ m s}^{-1}$ and [DIC] = 4.8 mol m^{-3} . This concept can be extended to our results by integrating the [DIC] with Eq. 2 and plotting J_{obs}

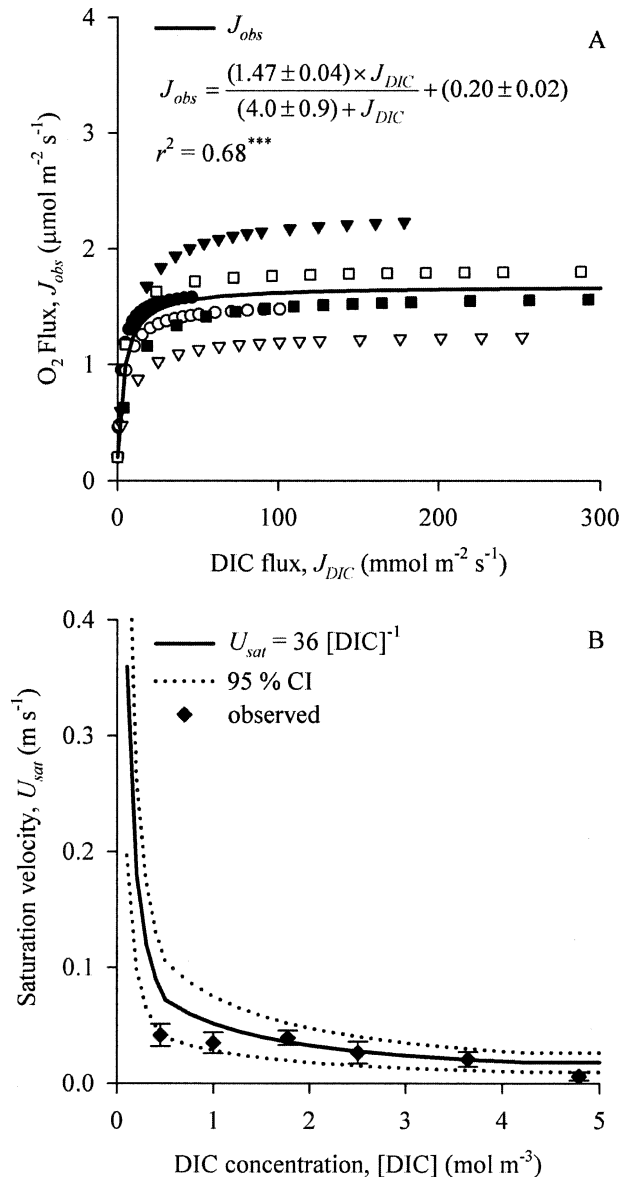


Fig. 10. (A) A model of the O_2 flux (J_{obs}) from a *V. americana* leaf with increasing rates of DIC flux, where $J_{obs} = \frac{J_{max} \times J_{DIC}}{V_{DIC} + J_{DIC}} + J_{diff}$. (B) A model of the relationship between the saturation velocity (U_{sat}) and [DIC], using the model presented in (A).

as a function of DIC flux (J_{DIC}) (Fig. 10A). It is evident that a rectangular hyperbola can be used to model the data, when $U < U_{crit}$ (note that $U < U_{crit}$ in our study). The half-saturation constant was $4.0 \pm 0.1 \text{ mmol m}^{-2} \text{ s}^{-1}$ and the average maximum O_2 flux ($\overline{J_{max}}$) was $1.47 \pm 0.04 \text{ } \mu\text{mol m}^{-2} \text{ s}^{-1}$, which provides a saturating J_{DIC} of $36 \text{ mmol m}^{-2} \text{ s}^{-1}$ (i.e., $9 \times$ the half-saturation constant). Given that the saturating J_{DIC} is a product of U_{sat} and [DIC], the relationship between U_{sat} and [DIC] can be modeled as $U_{sat} = 36 [\text{DIC}]^{-1}$. A reconsideration of the U_{sat} data presented in Figs. 3 and 4 confirms that the [DIC] examined in this study was not limiting (Fig. 10B).

This type of mass balance has significant implications for nutrient delivery to aquatic organisms as Sanford and Crawford (2000) described in their mechanistic model. However, their model did not predict the mass transfer limitation in this study. Rather, the Sanford and Crawford (2000) model predicted kinetic limitation at all U and DIC concentrations, which was not the case for the results in Fig. 3, where kinetic limitation occurred only when $U > U_{sat}$. We believe that this discrepancy is attributable to the limitation of the Sanford and Crawford (2000) model to account for the complex nature of the $\text{CO}_2\text{-HCO}_3^-$ reaction and DIC uptake mechanisms in aquatic macrophytes. Further refinement of their model is therefore warranted.

The CO_2 flux examined in this study was not sufficient to saturate J_{obs} (Fig. 7), which supports the hypothesis that CO_2 concentrations are limiting in aquatic ecosystems (Riebesell et al. 1993; McConnaughey 1998). Conversely, the HCO_3^- flux of [DIC] was always in excess (Fig. 8) for $U > U_{sat}$ and [DIC] did not limit J_{obs} at any of the concentrations examined (Fig. 3). Similar patterns were also found in the red algae *Gracilaria conferta*, where the surface concentration of HCO_3^- was $> 90\%$ of the bulk concentration (Gonen et al. 1995). Traditionally, it is assumed that $>90\%$ of the resistance to mass transfer is caused by resistance by the boundary layer (Madsen and Sand-Jensen 1991), hence the common assumption that surface concentrations of nutrients are zero (i.e., a perfect sink) (Wheeler 1980; Hurd et al. 1996). However, in this study HCO_3^- uptake was not limited (i.e., $C_s \neq 0$), especially at the lowest U (0.005 m s^{-1}) and [DIC] (0.46 mol m^{-3}) indicating that boundary layer resistance was negligible. Other factors that potentially provide resistance to the uptake of DIC by the plant are the mechanisms of DIC uptake (Price and Badger 2002), the conversion of HCO_3^- to CO_2 (McConnaughey 1998; Frost-Christensen et al. 2003), and mass transfer through cuticular membranes (i.e., O_2 mass transfer coefficients range from 1 to $40 \times 10^{-6} \text{ m s}^{-1}$; Frost-Christensen et al. 2003). The similar order of the mass transfer coefficients for cuticular membranes and concentration boundary layers suggest similar degrees of resistance. The question remains open on whether internal (i.e., cellular and molecular) resistances govern HCO_3^- uptake or if photosynthesis (or some related mechanism) is limiting. Clearly, biological, chemical, and physical resistance all serve to limit HCO_3^- uptake by aquatic macrophytes (Raven 1991; Tortell et al. 1997; Madsen and Maberly 2002).

The results of the study indicate that HCO_3^- uptake accounts for $>90\%$ of DIC uptake at low U with the contribution decreasing with U (Fig. 7). It is likely that DIC is not a limiting nutrient for HCO_3^- -users, because even at low [DIC], mass transfer provides sufficient carbon where $U < U_{sat}$. The proportionately greater HCO_3^- uptake rates at low U would help to provide a mechanism to explain the observation that HCO_3^- -using freshwater macrophytes dominate in slow flow environments (Raven 1991). Water motion does not appear to be a prerequisite for photosynthesis, as J_{obs} was observed in stagnant water in our study and in the study of the green algae *U. lactuca*

(Koch 1993). However, high velocities may inhibit photosynthesis, as has been observed in the freshwater angiosperm *C. stagnalis* at velocities $>0.012 \text{ m s}^{-1}$ (Madsen and Søndergaard 1983) (Fig. 1). It is evident that the maximum velocity used in our study was much less than the U_{crit} for *V. americana*.

Mass transfer—The simple flat morphology of *V. americana* enables direct comparisons of mass transfer to flat plate theory. Estimates of the Sh_x from hydrodynamic measurements compared well to those calculated from flat plate theory (Fig. 5) when the parameter a was set to that of constant surface flux (0.464). Specifically, these results confirm that theoretical predictions are borne out by hydrodynamic measurements. However, the theoretical predictions do not support the measurements of the scalar quantities in the CBL, which in the case of the δ_{CBL} and δ_{DSL} were $<63\%$ and $<70\%$, respectively, of what was predicted. This is even smaller than the 30% difference observed on sediments (Hondzo et al. 2005). Clearly, part of this discrepancy is because of the “biology” of the boundary conditions around *V. americana* leaves. The experimentally determined Sh_x from O_2 profiles were greater than that predicted by flat plate theory, and the parameter a (a function of the geometry, orientation, and boundary conditions) was 4.9 times higher ($a = 2.24 \pm 1.32$) than the value for constant surface flux. Whether 2.24 is the correct value for photosynthetic organisms remains to be determined for other species. Whereas it is possible that the O_2 microsensor disturbs the boundary layer and may enhance flux (Glud et al. 1994; Lorenzen et al. 1995), hydrodynamic measurements (Hondzo et al. 2005) and comparisons of O_2 flux made independently from an integrative technique (Nishihara and Ackerman 2006) suggest this to be negligible. Therefore, it can be inferred, from the large value of a , that physiochemical reactions occurring in the CBL or at the surface of the organism enhance the O_2 flux from the leaf by supplying CO_2 through active HCO_3^- uptake and/or the conversion of HCO_3^- to CO_2 (Tortell et al. 1997; Bozzo et al. 2000). Indeed, a reaction term (R) (e.g., Wolf-Gladrow and Reibesell 1997) should be included in Eq. 3 (Bird et al. 2002), and a good estimate of the reaction term should theoretically enable an analytical solution to the O_2 profile and provide more accurate measurements of O_2 flux and Sh_x (Bird et al. 2002).

By investigating how water velocity and nutrient concentrations combine to affect the photosynthesis and nutrient uptake rates of *V. americana*, this study shows that for low nutrient concentrations, water velocity has an important influence on photosynthesis and uptake rates, whereas at high nutrient concentrations water velocity was less important. The predictions of mass transfer by flat plate theory underestimated the values that were observed experimentally. Moreover, the Sanford and Crawford (2000) model on mass transfer and nutrient uptake is not applicable to DIC uptake. It is evident that DIC is not limiting for HCO_3^- -using photosynthetic organisms (Raven and Falkowski 1999). The recent discovery of active HCO_3^- uptake in diatoms, which are found in relatively low Reynolds number environments (Tortell et al. 1997)

supports this assertion. In such environments, the ability to acquire carbon from HCO_3^- would be advantageous since there is proportionately more HCO_3^- than CO_2 in natural waters (Raven and Falkowski 1999). Future studies should address how different plant morphologies affect the mass transfer of solutes to aquatic macrophytes and examine the full extent of the ecophysiological models.

References

- ACKERMAN, J. D., AND T. M. HOOVER. 2001. Measurement of local bed shear stress in streams using a Preston-static tube. *Limnol. Oceanogr.* **46**: 2080–2087.
- AMERICAN WATER WORKS ASSOCIATION. 1998. Standard methods for the examination of water and wastewater, 20th ed. United Book Press.
- BASMADJIAN, D. 2003. Mass transfer: Principles and applications. CRC Press LLC.
- BIRD, R. B., W. E. STEWART, AND E. N. LIGHTFOOT. 2002. Transport phenomena, 2nd ed. Wiley.
- BORCHARDT, M. A., J. P. HOFFMANN, AND P. W. COOK. 1994. Phosphorus uptake kinetics of *Spirogyra fluviatilis* (Charophyceae) in flowing water. *J. Phycol.* **30**: 403–417.
- BOZZO, G. G., B. COLMAN, AND Y. MATSUDA. 2000. Active transport of CO_2 and bicarbonate is induced in response to external CO_2 concentration in the green alga *Chlorella kessleri*. *J. Exp. Bot.* **51**: 1341–1348.
- CATLING, P. M., K. W. SPICER, M. BIERNACKI, AND J. L. DOUST. 1994. The biology of Canadian weeds. 103. *Vallisneria americana* Michx. *Can. J. Plant Sci.* **74**: 883–891.
- CORNELISEN, C. D., AND F. I. M. THOMAS. 2004. Ammonium and nitrate uptake by leaves of the seagrass *Thalassia testudinum*: Impact of hydrodynamic regime and epiphyte cover on uptake rates. *J. Mar. Syst.* **49**: 177–194.
- DADE, W. B. 1993. Near-bed turbulence and hydrodynamic control of diffusional mass transfer at the sea floor. *Limnol. Oceanogr.* **38**: 52–69.
- FALTER, J. L., M. J. ATKINSON, AND C. F. M. COIMBRA. 2005. Effects of surface roughness and oscillatory flow on the dissolution of plaster forms: Evidence for nutrient mass transfer to coral reef communities. *Limnol. Oceanogr.* **50**: 246–254.
- FLORES-MOYA, A. AND J. A. FERNÁNDEZ. 1998. The role of external carbonic anhydrase in the photosynthetic use of inorganic carbon in the deep-water alga *Phyllariopsis pupurascens* (Laminariales, Phaeophyta). *Planta*. **207**: 115–119.
- FROST-CHRISTENSEN, H., L. B. JØRGENSEN, AND F. FLOTO. 2003. Species specificity of resistance to oxygen diffusion in thin cuticular membranes from amphibious plants. *Plant Cell Environ.* **26**: 561–569.
- GLUD, R. N., J. K. GUNDERSEN, N. P. REVSBECH, AND B. B. JØRGENSEN. 1994. Effects on the benthic diffusive boundary layer imposed by microelectrodes. *Limnol. Oceanogr.* **39**: 462–467.
- GONEN, Y., E. KIMMEL, AND M. FRIEDLANDER. 1995. Diffusion boundary layer transport in *Gracilaria conferta* (Rhodophyta). *J. Phycol.* **31**: 768–773.
- HONDZO, M., T. FEYAERTS, R. DONOVAN, AND B. L. O'CONNOR. 2005. Universal scaling of dissolved oxygen distribution at the sediment-water interface: A power law. *Limnol. Oceanogr.* **50**: 1667–1676.
- HURD, C. L. 2000. Water motion, marine macroalgal physiology, and production. *J. Phycol.* **36**: 453–472.
- , P. J. HARRISON, AND L. D. DRUEHL. 1996. Effect of seawater velocity on inorganic nitrogen uptake by morphologically distinct forms of *Macrocystis integrifolia* from wave-sheltered and exposed sites. *Mar. Biol.* **126**: 205–214.
- INVERS, O., R. C. ZIMMERMAN, R. S. ALBERTE, M. PEREZ, AND J. ROMERO. 2001. Inorganic carbon sources for seagrass photosynthesis: An experimental evaluation of bicarbonate use in species inhabiting temperature waters. *J. Exp. Mar. Biol. Ecol.* **265**: 203–217.
- KOCH, E. W. 1993. The effect of water flow on photosynthetic processes of the alga *Ulva lactuca* L. *Hydrobiologia* **260/261**: 457–462.
- LARNED, S. T., V. I. NIKORA, AND B. J. F. BIGGS. 2004. Mass-transfer-limited nitrogen and phosphorus uptake by stream periphyton: A conceptual model and experimental evidence. *Limnol. Oceanogr.* **49**: 1992–2000.
- LORENZEN, J., R. N. GLUD, AND N. P. REVSBECH. 1995. Impact of microsensor-caused changes in diffusive boundary layer thickness on O_2 profiles and photosynthetic rates in benthic communities of microorganisms. *Mar. Ecol. Prog. Ser.* **119**: 237–241.
- LORKE, A., B. MÜLLER, M. MAERKI, AND A. WÜEST. 2003. Breathing sediments: The control of diffusive transport across the sediment-water interface by periodic boundary-layer turbulence. *Limnol. Oceanogr.* **48**: 2077–2085.
- MADSEN, T. M., AND S. C. MABERLY. 2002. Freshwater angiosperm carbon concentrating mechanisms: Processes and patterns. *Funct. Plant. Biol.* **29**: 393–405.
- , ———, AND G. BOWES. 1996. Photosynthetic acclimation of submersed angiosperms to CO_2 and HCO_3^- . *Aqua. Bot.* **53**: 15–30.
- , AND K. SAND-JENSEN. 1991. Photosynthetic carbon assimilation in aquatic macrophytes. *Aquat. Bot.* **41**: 5–40.
- , AND M. SØNDERGAARD. 1983. The effects of current velocity on the photosynthesis of *Callitriche stagnalis* Scop. *Aquat. Bot.* **15**: 187–193.
- MCCONNAUGHEY, T. 1998. Acid secretion, calcification, and photosynthetic carbon concentrating mechanisms. *Can. J. Bot.* **76**: 1119–1126.
- MEAD, R., R. N. CURNOW, AND A. M. HASTED. 2003. Statistical methods in agricultural and experimental biology, 3rd ed. CRC Press LLC.
- NISHIHARA, G. N., AND J. D. ACKERMAN. 2006. On the determination of mass transfer in a concentration boundary layer. *Limnol. Oceanogr. Methods* **4**: in press.
- NISHIZAKI, M. T., AND J. D. ACKERMAN. 2005. A secondary chemical cue facilitates juvenile-adult postsettlement associations in red sea urchins. *Limnol. Oceanogr.* **50**: 354–362.
- OKUBO, A., J. D. ACKERMAN, AND D. P. SWANEY. 2002. Passive diffusion in ecosystems, p. 31–106. *In* A. Okubo and S. A. Levin [eds.], Diffusion and ecological problems: New perspectives, 2nd ed. Springer.
- PLOUG, H., S. HIETANEN, AND J. KUPARINEN. 2002. Diffusion and advection within and around sinking, porous diatom aggregates. *Limnol. Oceanogr.* **47**: 1129–1136.
- , W. STOLTE, E. H. G. EPPING, AND B. B. JØRGENSEN. 1999. Diffusive boundary layers, photosynthesis, and respiration of the colony-forming plankton algae, *Phaeocystis* sp. *Limnol. Oceanogr.* **44**: 1949–1958.
- , ———, AND B. B. JØRGENSEN. 1999. Diffusive boundary layer of the colony-forming plankton alga *Phaeocystis* sp. — implications for nutrient uptake and cellular growth. *Limnol. Oceanogr.* **44**: 1959–1967.
- PRICE, G. D., AND M. R. BADGER. 2002. Advances in understanding how aquatic photosynthetic organisms utilize sources of inorganic carbon for CO_2 fixation. *Funct. Plant. Biol.* **29**: 117–121.
- PRINS, H. B. A., J. F. H. SNEL, R. J. HELDER, AND P. E. ZANSTRA. 1980. Photosynthetic HCO_3^- utilization and OH^- excretion in aquatic angiosperms. *Plant. Physiol.* **66**: 818–822.

- RAVEN, J. A. 1991. Implications of inorganic carbon utilization: Ecology, evolution, and geochemistry. *Can. J. Bot.* **69**: 908–924.
- . 2003. Inorganic carbon concentrating mechanisms in relation to the biology of algae. *Photosynth. Res.* **77**: 155–171.
- , AND P. G. FALKOWSKI. 1999. Oceanic sinks for atmospheric CO₂. *Plant Cell Environ.* **22**: 741–755.
- RIEBESELL, U., D. A. WOLF-GLADROW, AND V. SMETACEK. 1993. Carbon dioxide limitation of marine phytoplankton growth rates. *Nature* **361**: 249–251.
- SANFORD, L. P., AND S. M. CRAWFORD. 2000. Mass transfer versus kinetic control of uptake across solid-water boundaries. *Limnol. Oceanogr.* **45**: 1180–1186.
- SCHLICHTING, H., AND K. GERSTEN. 2000. *Boundary-layer theory*, 8th ed. Springer.
- SCHUEPP, P. H. 1993. Leaf boundary layers. *New Phytol.* **125**: 477–507.
- STEWART, H. L., AND R. C. CARPENTER. 2003. The effects of morphology and water flow on photosynthesis of marine macroalgae. *Ecology* **84**: 2999–3012.
- STUMM, W., AND J. J. MORGAN. 1996. *Aquatic chemistry*, 3rd ed. Wiley.
- THOMAS, F. I. M., AND M. J. ATKINSON. 1997. Ammonium uptake by coral reefs: Effects of water velocity and surface roughness on mass transfer. *Limnol. Oceanogr.* **42**: 81–88.
- , C. D. CORNELISEN, AND J. M. ZANDE. 2000. Effects of water velocity and canopy morphology on ammonium uptake by seagrass communities. *Ecology* **81**: 2704–2713.
- TITUS, J. E., AND W. H. STONE. 1982. Photosynthetic responses of two submerged macrophytes to dissolved inorganic carbon concentration and pH. *Limnol. Oceanogr.* **27**: 151–160.
- TORTELL, P. D., AND F. M. M. MOREL. 2002. Sources of inorganic carbon for phytoplankton in the eastern Subtropical and Equatorial Pacific Ocean. *Limnol. Oceanogr.* **47**: 1012–1022.
- , J. R. REINFELDER, AND F. M. M. MOREL. 1997. Active uptake of bicarbonate by diatoms. *Nature* **390**: 243–244.
- WHEELER, W. N. 1980. Effect of boundary layer transport on the fixation of carbon by the giant kelp *Macrocystis pyrifera*. *Mar. Biol.* **56**: 103–110.
- WOLF-GLADROW, D., AND U. RIEBESELL. 1997. Diffusion and reactions in the vicinity of plankton: A refined model for inorganic transport. *Mar. Chem.* **59**: 17–34.

Received: 12 December 2005

Accepted: 9 July 2006

Amended: 14 July 2006